Fermilab FERMILAB-Pub-01/341-E November 2001

A Precise Determination of Electroweak Parameters in Neutrino-Nucleon Scattering

G. P. Zeller[5], K. S. McFarland[8,3], T. Adams[4], A. Alton[4], S. Avvakumov[8], L. de Barbaro[5], P. de Barbaro[8], R. H. Bernstein[3], A. Bodek[8], T. Bolton[4], J. Brau[6], D. Buchholz[5], H. Budd[8], L. Bugel[3], J. Conrad[2], R. B. Drucker[6], B. T. Fleming[2], R. Frey[6], J.A. Formaggio[2], J. Goldman[4], M. Goncharov[4], D. A. Harris[8], R. A. Johnson[1], J. H. Kim[2], S. Koutsoliotas[2], M. J. Lamm[3], W. Marsh[3], D. Mason[6], J. McDonald[7], C. McNulty[2], D. Naples[7], P. Nienaber[3], A. Romosan[2], W. K. Sakumoto[8], H. Schellman[5], M. H. Shaevitz[2], P. Spentzouris[2], E. G. Stern[2], N. Suwonjandee[1], M. Tzanov[7], M. Vakili[1], A. Vaitaitis[2], U. K. Yang[8], J. Yu[3], and E. D. Zimmerman[2]

[1] *University of Cincinnati, Cincinnati, OH 45221*
[2] *Columbia University, New York, NY 10027*
[3] *Fermi National Accelerator Laboratory, Batavia, IL 60510*
[4] *Kansas State University, Manhattan, KS 66506*
[5] *Northwestern University, Evanston, IL 60208*
[6] *University of Oregon, Eugene, OR 97403*
[7] *University of Pittsburgh, Pittsburgh, PA 15260*
[8] *University of Rochester, Rochester, NY 14627*

(October 30, 2001)

The NuTeV collaboration has extracted the electroweak parameter $\sin^2\theta_W$ from the measurement of the ratios of neutral current to charged current ν and $\overline{\nu}$ cross-sections. Our value, $\sin^2\theta_W{}^{(\mathrm{on-shell})} = 0.2277 \pm 0.0013(\mathrm{stat}) \pm 0.0009(\mathrm{syst})$, is three standard deviations above the standard model prediction. We also present a model independent analysis of the same data in terms of neutral-current quark couplings.

Neutrino-nucleon scattering is one of the most precise probes of the weak neutral current. The Lagrangian for weak neutral current ν–q scattering can be written at tree level as

$$\mathcal{L} = -\frac{G_F \rho_0}{\sqrt{2}} (\overline{\nu}\gamma^\mu (1-\gamma^5)\nu) \times \left(\epsilon_L^q \overline{q}\gamma_\mu (1-\gamma^5) q + \epsilon_R^q \overline{q}\gamma_\mu (1+\gamma^5) q\right), \quad (1)$$

where deviations from $\rho_0 = 1$ describe non-standard sources of SU(2) breaking, and $\epsilon^q_{L,R}$ are the chiral quark couplings. For the weak charged current, $\epsilon^q_L = I^{(3)}_{\rm weak}$ and $\epsilon^q_R = 0$, but for the neutral current ϵ^q_L and ϵ^q_R each contain an additional term, $-Q\sin^2\theta_W$, where Q is the quark's electric charge in units of e. By measuring ratios of the charged and neutral current processes on a hadronic target, one can thus extract $\sin^2\theta_W$ and ρ_0.

In the context of the standard model, this measurement of $\sin^2\theta_W$ is comparable in precision to direct measurements of M_W. Outside of the standard model, neutrino-nucleon scattering provides one of the most precise constraints on the weak couplings of light quarks, and tests the validity of electroweak theory in a range of momentum transfer far from M_Z. This process is also sensitive to non-standard interactions, including possible contributions from leptoquark and Z' exchange [1].

The ratio of neutral current to charged current cross-sections for either ν or $\overline{\nu}$ scattering from isoscalar targets of u and d quarks can be written as [2]

$$R^{\nu(\overline{\nu})} \equiv \frac{\sigma(\overset{(-)}{\nu} N \to \overset{(-)}{\nu} X)}{\sigma(\overset{(-)}{\nu} N \to \ell^{-(+)} X)} = (g_L^2 + r^{(-1)} g_R^2), \quad (2)$$

where

$$r \equiv \frac{\sigma(\overline{\nu}N \to \ell^+ X)}{\sigma(\nu N \to \ell^- X)} \sim \frac{1}{2}, \quad (3)$$

and $g^2_{L,R} = (\epsilon^u_{L,R})^2 + (\epsilon^d_{L,R})^2$. Corrections to Equation 2 result from the presence of heavy quarks in the sea, the production of heavy quarks in the target, higher order terms in the cross-section, and any isovector component of the light quarks in the target. In particular, in the case where a final-state charm quark is produced from a d or s quark in the nucleon, there are large uncertainties resulting from the mass suppression of the charm quark. This uncertainty has limited the precision of previous measurements of electroweak parameters in neutrino-nucleon scattering [3–5].

To reduce the effect of uncertainties resulting from charm production, Paschos and Wolfenstein [6] suggested consideration of the observable:

$$R^- \equiv \frac{\sigma(\nu_\mu N \to \nu_\mu X) - \sigma(\overline{\nu}_\mu N \to \overline{\nu}_\mu X)}{\sigma(\nu_\mu N \to \mu^- X) - \sigma(\overline{\nu}_\mu N \to \mu^+ X)} = \frac{R^\nu - r R^{\overline{\nu}}}{1-r} = (g_L^2 - g_R^2). \quad (4)$$

R^- is more difficult to measure than R^ν, primarily because the neutral current scatterings of ν and $\overline{\nu}$ yield identical observed final states which can only be distinguished through *a priori* knowledge of the initial state neutrino.

METHOD

High-purity ν and $\overline{\nu}$ beams were provided by the Sign Selected Quadrupole Train (SSQT) beamline at the Fermilab Tevatron during the 1996-1997 fixed target run. Neutrinos were produced from the decay of pions and kaons resulting from interactions of 800 GeV protons in a BeO target. Dipole magnets immediately downstream of the proton target bent pions and kaons of specified charge in the direction of the NuTeV detector, while oppositely charged and neutral mesons were stopped in beam dumps. The resulting beam was almost pure ν or $\overline{\nu}$, depending on the charge of the parent mesons. Anti-neutrino interactions comprised 0.03% of the neutrino beam events, and neutrino interactions 0.4% of the anti-neutrino beam events. In addition, the beams of almost pure muon neutrinos contained a small component of electron neutrinos (mostly from $K^\pm_{e3}$ decays) which created 1.7% of the observed interactions in the neutrino beam and 1.6% in the anti-neutrino beam.

Neutrino interactions were observed in the NuTeV detector [7], located 1450 m downstream of the proton target. The detector consisted of an 18 m long, 690 ton steel-scintillator target, followed by an iron-toroid spectrometer. The target calorimeter was composed of 168 (3m $\times$ 3m $\times$ 5.1cm) steel plates interspersed with liquid scintillation counters (spaced every two plates) and drift chambers (spaced every four plates). The scintillation counters provided triggering information as well as a measurement of the longitudinal interaction vertex, event length, and energy deposition. The mean position of hits in the drift chambers established the transverse vertex for the event. The toroid spectrometer, used to determine muon charge and momentum, also provided a measurement of the muon neutrino flux in charged current events. In addition, the detector was calibrated continuously through exposure to beams of hadrons, electrons, and muons over a wide energy range [7].

For inclusion in this analysis, events are required to deposit at least 20 GeV of visible energy ($E_{\rm cal}$) in the calorimeter, which ensures full efficiency of the trigger, allows an accurate vertex determination, and reduces cosmic ray background. Events with $E_{\rm cal} > 180$ GeV are also removed. Fiducial criteria restrict the location of the neutrino interaction to the central region of the calorimeter. The chosen fiducial volume enhances interactions that are contained in the calorimeter, and minimizes the fraction of events from electron neutrinos or non-neutrino sources. After all selections, the resulting data sample consists of 1.62×10^6 ν and 0.35×10^6 $\overline{\nu}$ events with a mean visible energy ($E_{\rm cal}$) of 64 GeV and 53 GeV, respectively.

In order to extract $\sin^2\theta_W$, the observed neutrino events must be separated into charged current (CC) and neutral current (NC) candidates. Both CC and NC neutrino interactions initiate a cascade of hadrons in the target that is registered in both the scintillation counters and drift chambers. Muon neutrino CC events are distinguished by the presence of a final state muon that typically penetrates beyond the hadronic shower and deposits energy in a large number of consecutive scintillation counters. NC events usually have no final state muon and deposit energy over a range of counters typical of a hadronic shower.

These differing event topologies enable the statistical separation of CC and NC neutrino interactions based solely on event length. For each event, this length is defined by the number of scintillation counters between the interaction vertex and the last counter consistent with at least single muon energy deposition. Events with a "long" length are identified as CC candidates, while "short" events are most likely NC induced. The separation between short and long events is made at 16 counters ($\sim$ 1.7m of steel) for $E_{\rm cal} < 55$ GeV, at 17 counters for $55 \leq E_{\rm cal} < 100$ GeV, and otherwise at 18 counters. The ratios of short to long events measured in the ν and $\overline{\nu}$ beams are:

$$R^{\nu}_{\rm exp} = 0.3916 \pm 0.0007 \text{ and } R^{\overline{\nu}}_{\rm exp} = 0.4050 \pm 0.0016. \quad (5)$$

$\sin^2\theta_W$ can be extracted directly from these measured ratios by comparison with a detailed Monte Carlo simulation of the experiment. The Monte Carlo must include neutrino fluxes, the neutrino cross-sections, and a detailed description of the detector response.

A detailed beam simulation is used to predict the ν and $\overline{\nu}$ fluxes. In particular, a precise determination of the electron neutrino contamination in the beam is essential. The ratios $R^{\nu}_{\rm exp}$ and $R^{\overline{\nu}}_{\rm exp}$ increase in the presence of electron neutrinos in the data sample because electron neutrino charged current interactions are almost always identified as neutral current interactions.

The bulk of the observed electron neutrinos, 93% in the ν beam and 70% in the $\overline{\nu}$ beam, result from $K^{\pm}_{e3}$ decays. The beam simulation can be tuned with high accuracy to describe ν_e and $\overline{\nu}_e$ production from charged kaon decay because the $K^{\pm}$ contribution is constrained by the observed ν_μ and $\overline{\nu}_\mu$ fluxes. Because of the precise alignment of the beamline elements and the low acceptance for neutral particles, the largest uncertainty in the calculated electron neutrino flux is the 1.4% uncertainty in the $K^{\pm}_{e3}$ branching ratio [8]. Other sources of electron neutrinos include neutral kaons, charmed hadrons, and muon decays, all of which have larger fractional uncertainties (10–20%). Finally, small uncertainties in the calibration of the calorimeter and the muon toroid affect the muon and electron neutrino flux measurements. Additional constraints from the data, including direct measurements of ν_e and $\overline{\nu}_e$ charged current events and measurements of ν_μ events in the $\overline{\nu}_\mu$ beam (which also result from charm and neutral kaon decay) [9] reduce the electron neutrino uncertainties. At the highest energies ($E_\nu > 350$ for ν_μ and $E_\nu > 180$ for ν_e), the beam Monte Carlo underpredicts the measured flux and is thus not used.

Neutrino-nucleon deep inelastic scattering processes are simulated using a leading order (LO) model for the cross-section augmented with longitudinal scattering and higher twist terms. The cross-section parameterization incorporates LO parton distribution functions (PDFs) from charged current data measured obtained with the same target and model as used in this experiment [10,11]. These PDFs include an external constraint on $\sigma^{\overline{\nu}}/\sigma^{\nu}$ [11]. Small modifications adjust the parton densities to produce the inherent up-down quark asymmetry consistent with muon scattering [12] and Drell-Yan [13] data. A LO analysis of $\overset{(-)}{\nu}\ N \rightarrow \mu^+\mu^- X$ events [14] provides the shape and magnitude of the strange sea. Mass suppression from charged current charm production is modeled using a LO slow rescaling formalism [15] whose parameters and uncertainties come from the same high-statistics $\mu^+\mu^-$ sample. A model for $c\overline{c}$ production is chosen to match EMC data [16]; it is assigned a 100% uncertainty. A global analysis [17] provides a parameterization of the longitudinal structure function, R_L, which is allowed to vary within its experimental and theoretical uncertainties. Electroweak and QED radiative corrections to the scattering cross-section are applied using code supplied by Bardin [18], and uncertainties are estimated by varying the parameters in these corrections.

The Monte Carlo must also accurately simulate the response of the detector to the products of neutrino interactions in the target. The critical parameters that must be modeled are the calorimeter response to muons, the measurement of the position of the neutrino interactions, and the range of hadronic showers in the calorimeter. Precise determination of these effects is made through extensive use of both neutrino and calibration beam data. Measured detector parameters are then varied within their uncertainties to estimate systematic errors.

An important test of the simulation is its ability to predict the length distribution of events. Figure 1 shows event length distributions in the final data sample compared to the Monte Carlo prediction for our measured value of $\sin^2\theta_W$. Events reaching the toroid, which comprise about 80% of the CC sample, have been left out for clarity, but are included in the normalization of the data. Excellent agreement within uncertainties is observed in the overlap region of long NC and short CC events.

RESULTS

Having precisely determined $R^{\nu}_{\rm exp}$, $R^{\overline{\nu}}_{\rm exp}$, and their predicted values as a function of electroweak parameters $\sin^2\theta_W$ and ρ_0, we proceed to extract the best values of $\sin^2\theta_W$ and ρ_0. This is done by means of a fit that also includes the slow-rescaling mass for charm production (m_c) with its *a priori* constraint from $\mu^+\mu^-$ data [14]. $R^{\overline{\nu}}$ is much less sensitive to $\sin^2\theta_W$ than R^{ν}, but both are sensitive to m_c and ρ_0.

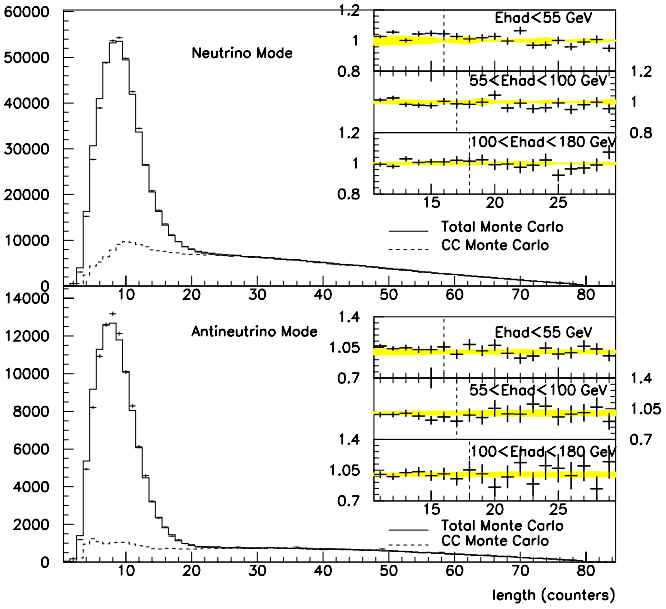

FIG. 1. Comparison of ν and $\overline{\nu}$ event length distributions in data and Monte Carlo (MC). The MC prediction for CC events is shown separately. Insets show data/MC ratio comparisons in the region of the length cut with bands to indicate the 1σ systematic uncertainty in this ratio.

SOURCE OF UNCERTAINTY	$\delta\sin^2\theta_W$	δR^ν	$\delta R^{\overline{\nu}}$
Data Statistics	0.00135	0.00069	0.00159
Monte Carlo Statistics	0.00010	0.00006	0.00010
TOTAL STATISTICS	0.00135	0.00069	0.00159
$\nu_e, \overline{\nu}_e$ Flux	0.00039	0.00025	0.00044
Energy Measurement	0.00018	0.00015	0.00024
Shower Length Model	0.00027	0.00021	0.00020
Counter Efficiency, Noise, Size	0.00023	0.00014	0.00006
Interaction Vertex	0.00030	0.00022	0.00017
TOTAL EXPERIMENTAL	0.00063	0.00044	0.00057
Charm Production, Strange Sea	0.00047	0.00089	0.00184
Charm Sea	0.00010	0.00005	0.00004
$\sigma^{\overline{\nu}}/\sigma^\nu$	0.00022	0.00007	0.00026
Radiative Corrections	0.00011	0.00005	0.00006
Non-Isoscalar Target	0.00005	0.00004	0.00004
Higher Twist	0.00014	0.00012	0.00013
R_L	0.00032	0.00045	0.00101
TOTAL MODEL	0.00064	0.00101	0.00212
TOTAL UNCERTAINTY	0.00162	0.00130	0.00272

TABLE I. Uncertainties for both the single parameter $\sin^2\theta_W$ fit and for the comparison of R^ν and $R^{\overline{\nu}}$ with model predictions.

When fitting with the assumption $\rho_0 = 1$, $\sin^2\theta_W$ is simultaneously fit with the slow-rescaling parameter m_c. Like an explicit calculation of R^-, this procedure reduces uncertainties related to sea quark scattering as well as many experimental systematics common to both ν and $\overline{\nu}$ samples. Statistical and systematic uncertainties in the $\sin^2\theta_W$ fit and in the comparison of R^ν and $R^{\overline{\nu}}$ with the Monte Carlo prediction are shown in Table I.

The single parameter fit for $\sin^2\theta_W$ measures:

$$\begin{aligned}\sin^2\theta_W^{(\mathrm{on-shell})} &= 0.2277 \pm 0.0013(\mathrm{stat.}) \pm 0.0009(\mathrm{syst.}) \\ &\quad - 0.00022 \times \left(\frac{M_{top}^2 - (175\,\mathrm{GeV})^2}{(50\,\mathrm{GeV})^2}\right) \\ &\quad + 0.00032 \times \ln\left(\frac{M_{Higgs}}{150\,\mathrm{GeV}}\right) \qquad (6)\end{aligned}$$

Leading terms in the one-loop electroweak radiative corrections [18] produce the small residual dependence of our result on M_{top} and M_{Higgs}. The prediction from a fit to other electroweak measurements is 0.2227 ± 0.00037 [19,20], approximately 3σ from our result. In the on-shell scheme, where $\sin^2\theta_W \equiv 1 - M_W^2/M_Z^2$, and where M_W and M_Z are the physical gauge boson masses, our result implies $M_W = 80.14 \pm 0.08$ GeV. The world-average of the direct measurements of M_W is 80.45 ± 0.04 GeV [19].

For the simultaneous fit to $\sin^2\theta_W$ and ρ_0, we obtain:

$$\rho_0 = 0.9983 \pm 0.0040,\ \sin^2\theta_W = 0.2265 \pm 0.0031, \qquad (7)$$

with a correlation coefficient of 0.85 between the two parameters. This suggests one but not both of $\sin^2\theta_W^{(\mathrm{on-shell})}$ or ρ_0 may be consistent with expectations. We have also performed a two-parameter fit in terms of the isoscalar combinations[1] of effective neutral-current quark couplings $(g_L^{\mathrm{eff}})^2$ and $(g_R^{\mathrm{eff}})^2$ at $\langle q^2 \rangle \approx -20$ GeV^2, which yields:

$$(g_L^{\mathrm{eff}})^2 = 0.3005 \pm 0.0014,\ (g_R^{\mathrm{eff}})^2 = 0.0310 \pm 0.0011, \qquad (8)$$

with a negligibly small correlation coefficient. A fit to predict these couplings from other electroweak data finds $(g_L^{\mathrm{eff}})^2 = 0.3042$ and $(g_R^{\mathrm{eff}})^2 = 0.0301$ [19,20].

In conclusion, NuTeV has made precise determinations of the electroweak parameters through separate measurements of R^ν and $R^{\overline{\nu}}$. We find a significant disagreement with the standard model expectation for $\sin^2\theta_W^{(\mathrm{on-shell})}$. In a model-independent analysis, this result suggests a smaller left-handed neutral current coupling to the light quarks than expected.

[1] Due to the asymmetry between the strange and charm seas and to the slight excess of neutrons in our target, this result is only sensitive to isovector combinations at about 3% of the sensitivity of isoscalar couplings.

ACKNOWLEDGEMENTS

We thank the staff of the Fermilab Beams, Computing and Particle Physics Divisions for design, construction, and operational assistance during the NuTeV experiment. This work was supported by the U.S. Department of Energy, the National Science Foundation and the Alfred P. Sloan foundation.

---

[1] P. Langacker *et al.* , Rev. Mod. Phys. **64**, 87 (1991).
[2] C. H. Llewellyn Smith, Nucl. Phys. **B228**, 205 (1983).
[3] K. S. McFarland *et al.* , Eur. Phys. Jour. **C1**, 509 (1998).
[4] A. Blondel *et al.* , Zeit. Phys. **C45**, 361 (1990).
[5] J. Allaby *et al.* , Zeit. Phys. **C36**, 611 (1985).
[6] E. A. Paschos and L. Wolfenstein Phys. Rev. **D7**, 91 (1973).
[7] D. A. Harris, J. Yu *et al.* , Nucl. Instr. Meth. **A447**, 373 (2000).
[8] D. E. Groom *et al.* , Eur. Phys. Jour. **C15**, 1 (2000).
[9] A. Alton *et al*., Phys. Rev. **D64**, 012002 (2001).
[10] A. J. Buras and K. J. F. Gaemers, Nucl. Phys. **B132**, 249 (1978).
[11] U. K. Yang *et al.*, Phys. Rev. Lett. **86**, 2742 (2001).
[12] M. Arneodo *et al.*, Nucl. Phys. **B487**, 3 (1997).
[13] E. A. Hawker *et al.*, Phys. Rev. Lett. **80**, 3715 (1998).
[14] M. Goncharov *et al*., eprint hep-ex/0102049, submitted to PRD, February 2001.
[15] R. M. Barnett, Phys. Rev. Lett. **36**, 1163 (1976).
[16] J. J. Aubert *et al.*, Nucl. Phys. **B213**, 31 (1983).
[17] L. W. Whitlow, SLAC-REPORT-357, 109 (1990).
[18] D. Yu. Bardin and V. A. Dokuchaeva, JINR-E2-86-260, (1986).
[19] "A Combination of Preliminary Electroweak Measurements and Constraints on the Standard Model", LEPEWWG/2001-01 (unpublished)
[20] M. Gruenewald, private communication, for the fit of Ref. [19] without the NuTeV preliminary result included.